General Relativity and Gravitation, Vol. 24, No. 7, 1992

Chaotic Motion of Test Particles in the Ernst Space-time

V. Karas[1] and D. Vokrouhlický[1]

Received August 7, 1991

Trajectories of test particles in the Ernst space-time are studied. The Poincaré surfaces of section are constructed and Lyapunov characteristic exponents are evaluated for a selected set of trajectories. This approach indicates that the number of isolating integrals is not sufficient to separate equations of motion and the particle trajectories are not integrable.

1.INTRODUCTION

The Ernst metric [1] is a static, axially symmetric, electro-vacuum solution of the Einstein–Maxwell equations with a black hole immersed in a magnetic field. Two parameters describe the solution: mass parameter M, and magnetic field parameter B_0. Setting $B_0 = 0$, $M \neq 0$, the Ernst metric reduces to the Schwarzschild metric, while with $B_0 \neq 0$, $M = 0$ we obtain Melvin's magnetic universe. The Ernst solution has been generalized to a class of magnetized Kerr–Newman solutions [2] and its possible astrophysical applications have been discussed by several authors [3,4]. Complete understanding of the space-time structure, however, has not been achieved even in the simplest case of the static solution, probably for two main reasons: (i) The Ernst solution is not asymptotically flat, and (ii) the geodesic equation has not been successfully separated and solved as yet. Several authors studied special cases of the test particle motion [5–12]. Equatorial

[1] Department of Astronomy and Astrophysics, Charles University, Švédská 8, 150 00 Prague, Czechoslovakia. e-mail: jana@cspuni12.bitnet

0001-7701/92/0700-0729$06.50/0

orbits and their perturbations were discussed in detail but very little is known about non-equatorial trajectories.

In this paper, we study test motion of both electrically charged and neutral particles. In particular, we address the problem of the existence or non-existence of an additional constant of motion (analogous to Carter's constant in the Kerr space-time). Our approach is mainly numerical and we basically follow the well-known paper by Hénon and Heiles [13], who studied the chaotic motion in a configuration with the same number of degrees of freedom as in our case (2), but with a different form of the potential. We also evaluate Lyapunov characteristic exponents (LCE) of a set of trajectories with various energies and initial conditions. Several issues in the conception of LCE within the framework of general relativity are discussed.

With some minor restrictions (given by the applicability of the numerical method) we conclude that no additional constant of motion exists and the equation of the test particle motion cannot thus be separated in general. Such a negative conclusion can be expected because equations of motion are integrable in very special cases only. However, we believe that the result is of interest at least for two reasons: (i) magnetized black holes are perhaps the simplest exact solutions generalizing ordinary black hole spacetimes with no singularities outside the horizon, and (ii) the method of LCE and related techniques was found very powerful in variety of situations where a quantitative definition of stochasticity of orbits is needed. On the other hand, it has not been frequently used within the area of general relativity.

2. TRAJECTORIES OF TEST PARTICLES

The metric of the Ernst solution in Schwarzschild-like coordinates with geometrical units is

$$ds^2 = \Lambda^2 \left(\frac{\Delta}{r^2} dt^2 - \frac{r^2}{\Delta} dr^2 - r^2 d\theta^2 \right) - \Lambda^{-2} r^2 \sin^2\theta d\phi^2, \qquad (1)$$

where $\Delta = r^2 - 2Mr$ and $\Lambda = 1 + \frac{1}{4} B_0^2 r^2 \sin^2\theta$. The electromagnetic field four-potential has a non-zero component

$$A_\phi = -\tfrac{1}{2} B_0 \Lambda^{-1} r^2 \sin^2\theta. \qquad (2)$$

The equation of motion of a test particle with rest mass m and electric charge q is given by

$$\frac{DU^\mu}{d\tau} = \frac{q}{m} F^\mu_\nu U^\nu, \qquad F_{\mu\nu} = A_{\nu,\mu} - A_{\mu,\nu}. \qquad (3)$$

In the hamiltonian formalism, eq. (3) can be derived from

$$\frac{d}{d\tau}x^\alpha = \frac{\partial \mathcal{H}}{\partial \pi_\alpha}, \qquad \frac{d}{d\tau}\pi_\alpha = -\frac{\partial \mathcal{H}}{\partial x^\alpha}, \tag{4}$$

where τ is an affine parameter along the trajectory (which can be chosen identical to the proper time) and

$$\mathcal{H} = \tfrac{1}{2} g^{\alpha\beta}\left(\pi_\alpha - qA_\alpha\right)\left(\pi_\beta - qA_\beta\right). \tag{5}$$

Evidently, three constants of motion can be found: the rest mass m of the particle, energy $\mathcal{E} \equiv P_t$, and projection of the generalized angular momentum onto the symmetry axis $\mathcal{L} \equiv P_\phi + qA_\phi$. The phase space of a particle moving under no constraints is 8-dimensional. Considering constants $\mathcal{E}$ and $\mathcal{L}$, the motion with respect to t and ϕ coordinates is separated and the number of degrees of freedom is reduced to 2. In the (r,θ)-plane the trajectory is bounded to a region which is determined by the condition $\mathcal{E} \geq V(r,\theta)$ with the effective potential

$$V(r,\theta) = \Lambda^2 \Delta r^{-2}\left[m^2 + \left(\frac{\Lambda}{r\sin\theta}\left(\mathcal{L} + qA_\phi\right)\right)^2\right]. \tag{6}$$

Boundaries of the region of allowed motion $[\mathcal{E} = V(r,\theta)]$ for several values of energy are shown in Fig. 1. Interestingly, a suitable choice of the parameters describing the metric (M, B_0) and the particle (m, q, $\mathcal{E}$, $\mathcal{L}$) gives two separated regions near the equatorial plane $\theta = \pi/2$. Both regions join together for $\mathcal{E} > \mathcal{E}_{\rm crit}$, as shown in the figure.

To find trajectories analytically (in the form analogous to, e.g., Carter's equations in the Kerr metric) another independent constant of motion is required. If such a constant existed, eq. (3) could be decoupled and separated. In the well-known case of the Kerr space-time the existence of Carter's constant is associated with the Killing–Yano tensor. However, the Ernst space-time is of the Petrov type I [14] in contrast to the type D of the Kerr metric, and therefore the existence of a non-trivial Killing–Yano tensor is excluded [15]. Unfortunately, there is no general, analytical method to find all constants of motion (except for those associated with evident symmetries of the metric) or at least to prove or disprove their existence [16].

Another approach to the problem, which is based on the numerical treatment, employs the methods of the Poincaré surfaces of section and LCE [13,16].

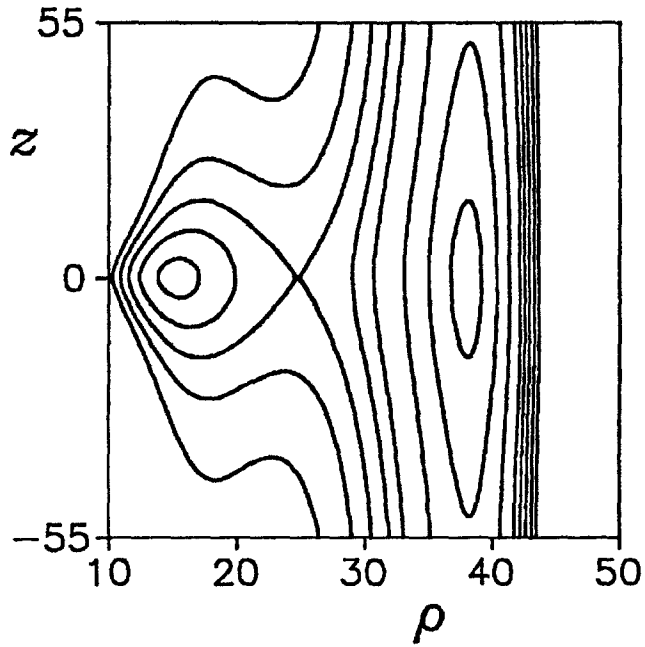

Fig. 1. The typical shape of the boundaries of allowed motion in the (z, ρ)-plane; $z = r\cos\theta$, $\rho = r\sin\theta$. In this figure, $B_0M = 0.15$, $q/m = 7.1$, $\mathcal{L}/m = -87.09$, and the curves are plotted for energy in the region $115 \leq \mathcal{E}/m \leq 134$ (the cusp occurs for $\mathcal{E}/m = 128.456$).

3. SURFACES OF SECTION

In the first method we choose a surface in the phase space ($\theta = \pi/2$, say) and plot cross sections of the trajectory in the graph with another two coordinates on the abscissa and ordinate, respectively (e.g. r and $\dot{r}$). There are basically no restrictions on the choice of the surface of section except one—it must not coincide with the hyper-surface of a constant of motion (also called the isolating integral). If the additional integral exists, the trajectory is bound to a hyper-surface in the phase space; this hyper-surface crosses the surface of section in a curve. In other words, crossings of the trajectory with a surface of section form a curve in the graph. For example, in the case of the Schwarzschild background metric [$B_0 = 0$ in (1)] this additional constant is obviously associated with the other components of the particle's angular momentum due to the spherical symmetry and we

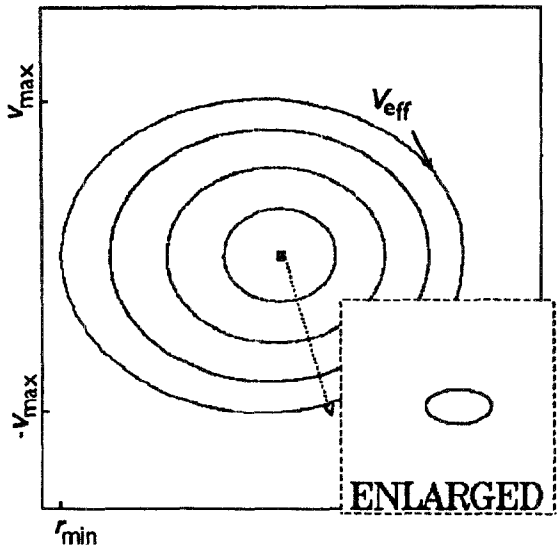

Fig. 2a

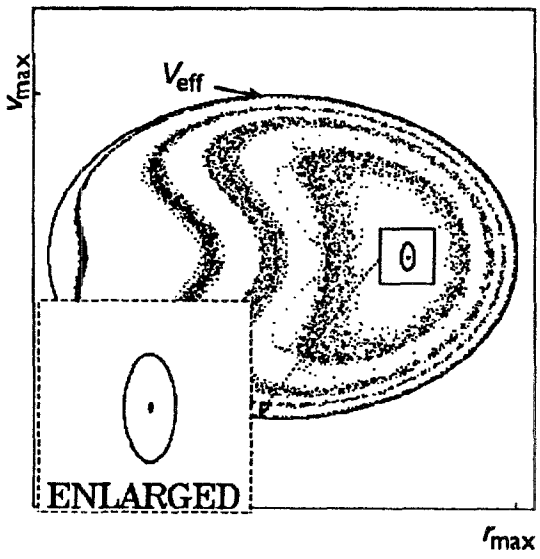

Fig. 2b

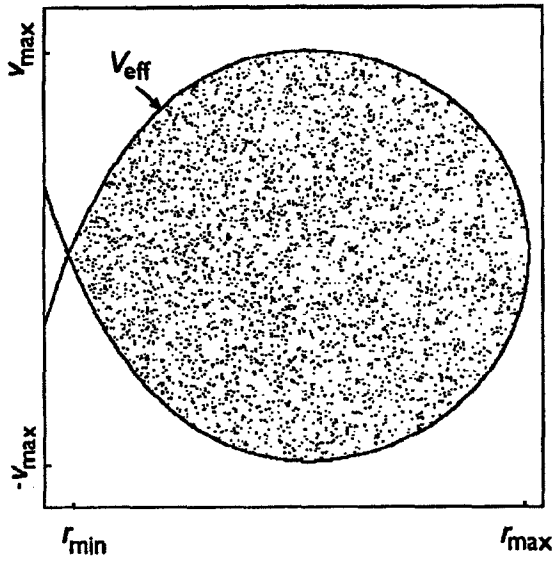

Fig. 2c

Fig. 2. The surfaces of section for electrically neutral particles with $B_0M = 0.15$, $\mathcal{L}/m = 25$ and different values of specific energy $\mathcal{E}/m$: (a) 5.01, (b) 5.1, and (c) 5.39687. Surfaces of section show typically stronger chaotic behaviour when the energy exceeds some value: In (a) the cross-sections corresponding to different initial conditions are fairly sharp and form separated curves, while in (c) they are distributed randomly through the allowable area. In this last case, a cusp in the $V_{\rm eff}$ curve forms at the inner radius $r_{\rm min}$. This corresponds to a critical, self-crossing equipotential surface with a Lagrangian point; if material fills this surface, the cusp will transfer mass to the black hole. (For details see the text.)

obtain

$$\left(v^r_{(\rm loc)}\right)^2 = 1 - \frac{\Delta}{r^2\mathcal{E}^2}\left(m^2 + \frac{l^2}{r^2}\right), \tag{7}$$

where

$$l^2 = \mathcal{L}^2 + \left(P_{\theta,(0)}\right)^2 .$$

(Note that we prefer to use the radial velocity measured by the local static observers located at the position of the particle, $v^r_{(\rm loc)}$, instead of $\dot{r}$.) Another limiting case of (1) corresponds to the cylindrically symmetric Melvin space-time [$M = 0$ in (1)] which is endowed with the additional Killing vector field ∂_z, $z = r\cos\theta$. The integrability is now ensured analogously to the Schwarzschild case. However, one cannot follow the same conception as with eq. (7) because the motion in the z-direction is unbounded.

On the other hand, if no additional constant of motion exists, we observe a fuzzy structure in the graph and the motion is called chaotic.

Figures 2 and 3 show several typical examples of surfaces of section in the case of electrically neutral and electrically charged particles, respectively. Cross sections of a trajectory in the phase space with the $\theta = \pi/2$ plane are plotted in the $(r, v^r_{(\mathrm{loc})})$-graph. The curve of the effective potential which bounds the cross sections in the graphs is marked V_{eff} and also plotted for given values of $\mathcal{E}$ and $\mathcal{L}$. In the case of electrically neutral particles this curve has topology of a circle; allowable area is then $r_{\min} \leq r/M \leq r_{\max}$ and $-v_{\max} \leq v^r_{(\mathrm{loc})} \leq v_{\max}$. As in Fig. 1, in the case of charged particles two separated regions may occur; in that case we restrict ourselves to one of the regions (the other region can be studied analogously). The graphs are constructed for several values of energy. In general, trajectories appear less chaotic when the energy is not too high; in that case, the set of points corresponding to a given trajectory covers only a small part of the allowable area (in the terminology of Ref. 13)—some points even seem to lie on a curve. 'Stochastic' trajectories appear separated by regular ones since two degrees of freedom of the problem do not allow the Arnold diffusion [16]. On the other hand, higher energy yields stochastic trajectories which fill a large portion of the allowable area and regular trajectories cannot be found.

4. LYAPUNOV CHARACTERISTIC EXPONENTS

The method of LCE provides us with a more quantitative description of the system with chaotic features. Although the method is again based on numerical evaluations and thus some critical remarks on its applicability must be accepted, it is closer to the rigorous prove of chaoticity (and thus non-integrability) than the previous approach. Roughly speaking, it is based on computing the mean rate of divergence of a bundle of orbits. A deep survey of the theory of Lyapunov exponents and their key role in the concept of stochasticity is given in [16,18,19]; numerical algorithms and recipes for their estimate can be found there as well. The following paragraph contains a very brief exposition of the formalism based mainly on [18].

4.1 Brief review of the theory

Within the framework of classical mechanics, the phase space of a dynamical system with n degrees of freedom is represented by a $2n$-dimensional manifold $\mathcal{M}$ (we assume $\mathcal{M}$ compact). Let us denote by Φ^t a flow which is a solution of the Hamilton equations. LCE are quasi-local quantities characterizing a curve η induced by Φ^t with given initial conditions at $t = 0$,

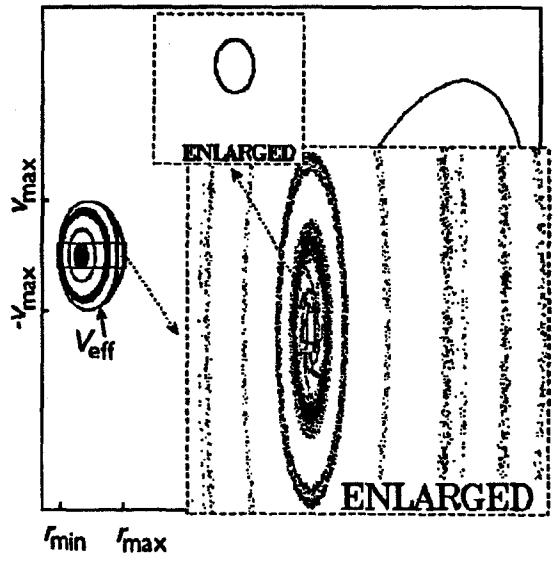
ENLARGED
v_{max}
$-v_{max}$
V_{eff}
ENLARGED
r_{min}
r_{max}

Fig. 3a

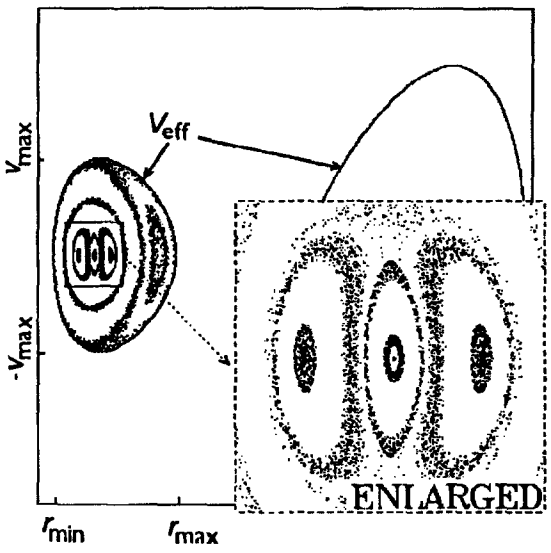
V_{eff}
v_{max}
$-v_{max}$
ENLARGED
r_{min}
r_{max}

Fig. 3b

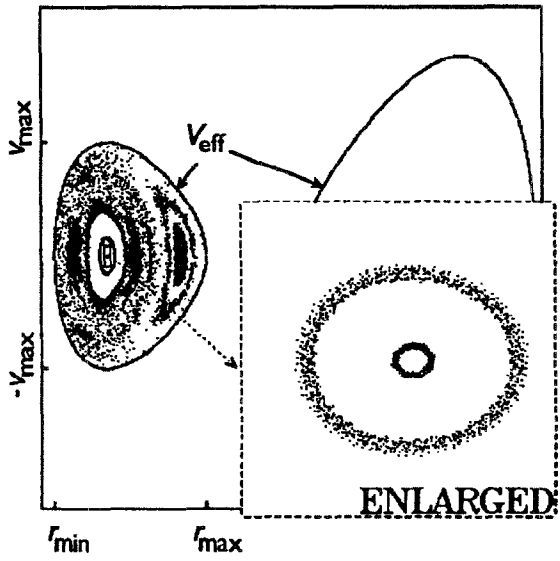

Fig. 3c

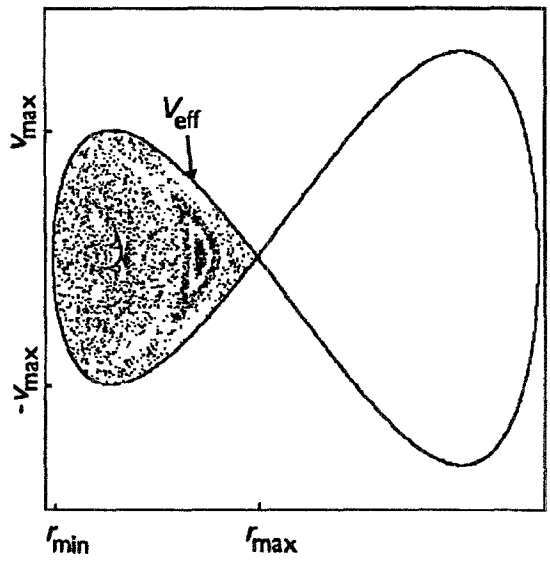

Fig. 3d

Fig. 3. The same as in Fig. 2, but for electrically charged particles with $\mathcal{L}/m = -87.09$, $q/m = 7.1$ and $\mathcal{E}/m$: (a) 11.14, (b) 11.235, (c) 11.284, and (d) 11.334.

$x \in \mathcal{M}$. Let $y(s)$ be a curve connecting $y(0) = x$ with another points on nearby curves of the flow. Let us denote by $\mathrm{T}_x\mathcal{M}$ tangent space at x,

$$w = \frac{\partial y}{\partial s}_{|s=0} \in \mathrm{T}_x\mathcal{M},$$

and by $d(\,,\,)$ the distance on $\mathcal{M}$ induced by the metric. Thus,

$$d(y(s), x) = s\|w\| + o(s).$$

Analogously for Φ-transported quantities

$$\mathrm{D}\Phi_x^t w = \frac{\partial \Phi^t y}{\partial s}_{|s=0} \in \mathrm{T}_{\Phi^t x}\mathcal{M}$$

$$d(\Phi^t y(s), \Phi^t x) = s\|\mathrm{D}\Phi_x^t w\| + o(s),$$

where $\mathrm{D}\Phi_x^t : \mathrm{T}_x\mathcal{M} \to \mathrm{T}_{\Phi^t x}\mathcal{M}$ is the linear mapping. Finally, the Lyapunov characteristic exponent relative to x and w is defined by

$$\gamma(x, w) \stackrel{\mathrm{def}}{=} \lim_{\substack{t\to\infty \\ s\to 0}} \frac{1}{t} \ln \frac{d(\Phi^t y(s), \Phi^t x)}{d(y(s), x)} = \lim_{t\to\infty} \frac{\|\mathrm{D}\Phi_x^t w\|}{\|w\|}. \qquad (8)$$

A non-zero LCE corresponds to trajectories diverging exponentially, as can be seen from (8). For the given flow curve η the value of $\gamma(x, w)$ is actually independent of x because we consider the limit $t \to \infty$. In the case of periodic orbits one can introduce the basis $\{\mathrm{e}_i\}$, $i = 1, \ldots, 2n$ of $\mathrm{T}_{\Phi^t x}\mathcal{M}$ constructed from eigenvectors of $\mathrm{D}\Phi_x^t$ and obtain $2n$ LCE $\gamma(\mathrm{e}_i)$ each of which is connected with one of the basis vectors. It can be proved that exactly $2n$ different LCE describe non-periodic orbits as well.

Several features of LCE will be important in the following. First, restricting to a k-dimensional subspace in $\mathrm{T}_{\Phi^t x}\mathcal{M}$ and evaluating $\gamma(w)$ for any w from this subspace one obtains just the maximum LCE associated with basis vectors of the subspace, $\gamma(\mathrm{e}_i)$. In other words, inserting an arbitrarily chosen vector $w \in \mathrm{T}_x\mathcal{M}$ in (8) one always obtains the maximum LCE (except for singular cases; for details refer to Refs. 16,18).

Next, for a Hamiltonian flow there is a symmetry in LCE which can be expressed in the form $\gamma(\mathrm{e}_i) = -\gamma(\mathrm{e}_{2n-i+1})$.

The key theorem on which our conclusions are based is due to Casati et al. [17] who proved that every isolating integral of motion decreases the number of non-zero LCEs by two. In particular, for integrable Hamiltonian systems the rate of divergence of nearby trajectories is polynomial at

maximum (not exponential) everywhere in the phase space and thus all the LCE vanish. From this point of view the indication of a non-zero Lyapunov exponent excludes global integrability of the problem. One has to stress the adjective 'global' in the previous statement because LCE are purely quasi-local quantities. They are associated with the given trajectory.

For practical determination of the maximum LCE on a computer one cannot follow the definition (8) immediately. According to one of the widely used methods which we also have employed, one starts with two close trajectories and follows them (by solving equations of motion numerically) until the separation exceeds some pre-determined upper value. The separation of trajectories is then scaled down to its initial value and the equations of motion are solved further with new starting conditions. (Equivalently, a constant time interval between rescalings can be given.) Therefore, the trajectories remain close to each other. The maximum LCE is determined as a numerically estimated limit

$$\gamma = \lim_{n\to\infty} \sum_{i=1}^{n} \frac{1}{t_i} \ln \frac{d_i}{d_0} ,$$

with d_0 and d_i lengths of separation vectors at initial time and at time t_i of i-th rescaling. The last expression for γ and the whole approach follows from the linearity of equations for deviations of infinitesimally close orbits.

4.2 LCE formulated within the 3 + 1 approach

Now we apply the approach of the previous paragraph to trajectories describing motion of test particles in a curved space-time. We wish to maintain an operationalist definition of LCE as a description of the relative motion along initially close trajectories as seen by a physical observer. Such a description comes naturally within the framework of the 3 + 1 formalism. Thus, we first choose a set of fiducial observers who measure space separations of the trajectories taking into account symmetries of the space-time.

In particular, we consider the static solution (1) of the Einstein–Maxwell equations. One can introduce a set of preferred static observers and estimate LCE on basis of separations in the phase space as measured by these observers in space-like hyper-surfaces $\mathcal{S}_t$ of constant global time t. (For a description of 3 + 1 splitting of the space-time we use here see, e.g., Ref. 20.) It can be seen (e.g., Refs. 16,18) that the value of LCE does not depend on metric in $\mathcal{S}_t$. Naturally, it does depend on the choice of fiducial observers themselves and this choice is not unique, however, in a static space-time a reasonable definition of these observers is possible.

3-dimensional vectors are obtained by projecting 4-dimensional quantities into $\mathcal{S}_t$ with the projection tensor $h^\mu_\nu = \delta^\mu_\nu + U^\mu U_\nu$, where U^μ denotes the observer's four-velocity: $\tilde{x}^i = h^i_\mu x^\mu$, $\tilde{\pi}_i = h^\nu_i \pi_\nu$. For the 3-metric corresponding to the space-time element (1) $\tilde{g}^{ij} = g^{ij}$, $\tilde{g}_{ij} = g_{ij}$ $(i,j = 1,\ldots,3)$. (Let us mention that in a non-relativistic limit with $B_0 = 0$ and $r \to \infty$ in (1) we obtain the standard definition of LCE.) Hamilton equations in 3-quantities have their standard form

$$\frac{d}{d\tau}\tilde{x}^\alpha = \frac{\partial \tilde{\mathcal{H}}}{\partial \tilde{\pi}_\alpha}, \qquad \frac{d}{d\tau}\tilde{\pi}_\alpha = -\frac{\partial \tilde{\mathcal{H}}}{\partial \tilde{x}^\alpha} \tag{9}$$

with

$$\tilde{\mathcal{H}} = \mathcal{H}(\tilde{x}^i, \tilde{\pi}_j; \pi_t \to \mathcal{E}). \tag{10}$$

One can see that $(\tilde{x}^i, \tilde{\pi}_j)$ are canonically conjugate variables in a 6-dimensional phase space $\mathcal{M}^{(6)}$ with hamiltonian flow induced by $\tilde{\mathcal{H}}$.

Obviously, two integrals of motion are present: $\tilde{\pi}_\phi = \mathcal{L}$ (projection of the angular momentum) and $\tilde{\mathcal{H}} = m^2$ (square of the rest mass of the particle). Due to these integrals four of the LCE are necessarily zero. It is only the remaining pair of them that could be non-zero. If this is the case, the non-zero LCE must have opposite signs because the problem is represented by the Hamiltonian flow in the phase space. To conclude, there remains only one independent, possibly non-zero LCE in our problem. This fact simplifies the required computations [16,18].

Figure 4 shows a numerically evaluated estimate of limiting values of LCE for a selected set of trajectories starting in the equatorial plane with radial coordinate r; λ is defined as

$$\lambda \stackrel{\text{def}}{=} \lim_{t\to\infty} \lambda(t) = \lim_{t\to\infty} \frac{\|\mathrm{D}\Phi^t_x w\|_{\mathrm{s}}}{\|w\|_{\mathrm{s}}},$$

where $\|\ \|_{\mathrm{s}}$ is the norm in the space part of $\mathrm{T}_x\mathcal{M}^{(6)}$. This limit is often non-zero, indicating non-zero γ and thus chaotic motion. To reach the plateau of the $\lambda(t)$ curve in the chaotic region, the number of time steps required in integration of one trajectory was typically 10^6–10^7. It is a well-known fact, which has already been discussed in the classic paper [13], that there can occur nearly regular islands in the developed chaotic sea in the phase space. Such islands exist in our problem too; they are indicated by a decrease of λ in Fig. 4. Particles moving along corresponding trajectories remain close each other and small values of λ indicate that LCE vanish. In the interval marked by arrows the divergence of orbits is much slower and the maximum value of the λ in this region does not exceed 10^{-8} (in

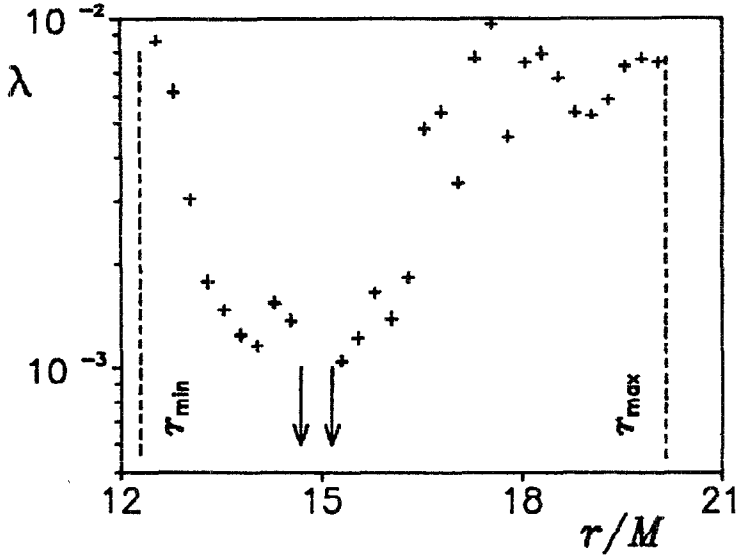

Fig. 4a

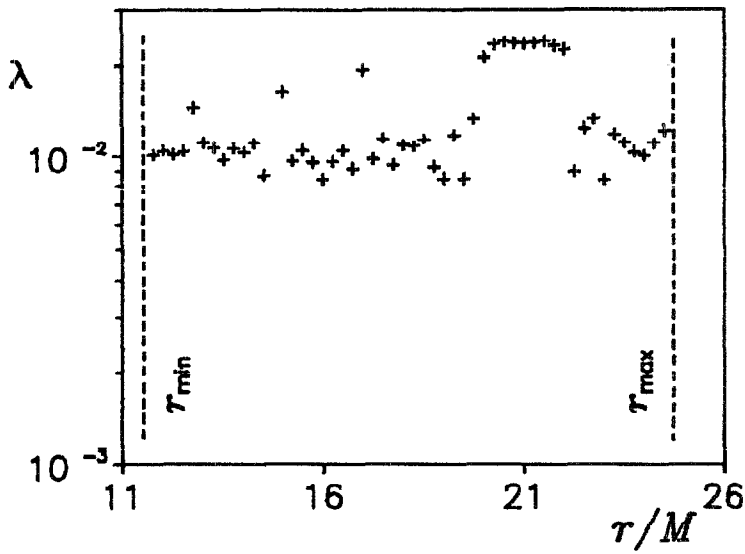

Fig. 4b

Fig. 4. Graphs (a) and (b) show terminal values of λ corresponding to the surfaces of section in Figs. 3 (b) and (d), respectively. Regions with chaotic trajectories are indicated by fuzzy structures in Fig. 3 and non-zero terminal values of λ in this figure. On the other hand, the arrows in Fig. 4a determine an upper estimate of λ in the region where trajectories diverge very slowly and appear nearly regular compared to other regions. Boundaries $r_{\min}$, $r_{\max}$ are determined by the effective potential [eq. (6)].

convenient units), as opposed to $\approx 10^{-2}$ in chaotic regions. (Analogously, no divergence can be detected for trajectories corresponding to those in Fig. 2a.) Note that Fig. 3 displays sharp structures where regular orbits are detected by vanishing λ.

5. CONCLUSIONS

5.1 Non-integrability of trajectories

In this paper we have studied, numerically, orbits of test particles in the Ernst space-time, constructed the Poincaré surfaces of section and estimated the value of LCE for a set of typical trajectories. Previous works on this subject have dealt mostly with orbits confined to the equatorial plane, because the equations of motion in a general case outside this plane have not been successfully separated and solved as yet. We conjecture that the separation is very probably impossible, because the motion of test particle appears to be chaotic.

5.2 Warnings

The objections against both numerical methods we have used arise from a principal impossibility of tracing the particle trajectory throughout an infinite time span. On the contrary, both non-integrability arguments are based on performing an infinite number of operations—either crossings of the particular trajectory with the surface of section or time steps in the series of rescalings according to the computer code for evaluation of LCE [16]. Here are the usual reasons for opposing the numerical approaches which one often faces:

1. One can always construct a curve joining all the crossings of the particle trajectory in the phase space with the surface of section because there is only a *finite* number of them.
2. The limit of a series is of course independent of a finite number of its terms, while within the framework of the numerical approach which we have employed only such a finite—though very large—number is evaluated.

Bearing this in mind, we suggest the strong evidence of non-integrability of the problem discussed here.

ACKNOWLEDGEMENTS

The authors thank M. Šidlichovský for helpful comments. We are also grateful to the referee for several suggestions which helped us to improve our manuscipt. This work was supported in part by the IBM Academic Initiative in Czechoslovakia.

REFERENCES

1. Ernst, F. J. (1976). *J. Math. Phys.* **17**, 54.
2. Bretón Baez, N., and García Díaz, A. (1986). *J. Math. Phys.* **27**, 562.
3. Dokuchaev, V. I. (1987). *Sov. Phys. JETP* **65**, 1079.
4. Karas, V., and Vokrouhlický, D. (1991). *J. Math. Phys.* **32**, 714.
5. Dadhich, N., Hoenselaers, C., and Vishveshwara, C. V. (1979). *J. Phys. A* **12**, 215.
6. Dhurandhar, S. V., and Sharma, D. N. (1983). *J. Phys. A* **16**, 99.
7. Esteban, E. P. (1984). *Nuovo Cimento B* **79**, 76.
8. Esteban, E. P. (1985). *Nuovo Cimento B* **87**, 35.
9. Aliev, A. N., and Gal'tsov, D. V. (1989). *Sov. Phys.–Usp.* **32**, 75.
10. Krori, K. D., Choudhury,, R., and Sarmah, J. C. (1986). *Can. J. Phys.* **64**, 1455.
11. Karas, V., and Vokrouhlický, D. (1990). *Class. Quant. Grav.* **7**, 391.
12. Vokrouhlický, D., and Karas, V. (1991). *Astron. Astrophys.* **243**, 165.
13. Hénon, M., and Heiles, C. (1964). *Astron. J.* **69**, 73.
14. Bose, S. K., and Esteban, E. (1981). *J. Math. Phys.* **22**, 3006.
15. Kramer, D., Stephani, H., MacCallum, M. A. H., and Herlt, E. (1980). *Exact Solutions of Einstein's Field Equations* (Cambridge University Press, Cambridge).
16. Lichtenberg, A. J., and Lieberman, M. A. (1983). *Regular and Stochastic Motion* (Springer-Verlag, New York).
17. Casati, G., Chirikov, B. V., and Ford, J. (1980). *Phys. Lett.* **77A**, 91.
18. Froeschlé, Cl. (1984). *Celest. Mech.* **34**, 95.
19. Benettin, G., Galgani, L., Giorgilli, A., and Strelcyn, J.-M. (1980). *Meccanica* March, 9.
20. Thorne, K. S., and Macdonald, D. A. (1982). *Mon. Not. R. Astr. Soc.* **198**, 339.